Supporting Information

Self-breathing strategy-enabled high-performance self-powered photoelectrochemical sensing by integrating with perovskite Ag_3BiO_3/Ti_3C_2 plasmonic heterojunction

Xiaojiao Du,[a] Xingyu Ji,[a] Wenhan Du[a] and Ding Jiang[b,*]

[a] School of Photoelectric Engineering, Changzhou Institute of Technology, Changzhou, Jiangsu, 213032, P. R. China

[b] Jiangsu Key Laboratory of Advanced Catalytic Materials and Technology, School of Petrochemical Engineering, Changzhou University, Changzhou, Jiangsu, 213164, P. R. China

∗Corresponding author.
Tel: +86 519 86330239
E-mail address: jiangding@cczu.edu.cn (D. Jiang)

Table of Contents

Experimental section.....**S3**

Fig. S1.....**S-6**

Fig. S2.....**S-7**

Fig. S3.....**S-8**

Fig. S4.....**S-9**

Fig. S5.....**S-10**

Fig. S6.....**S-11**

Fig. S7.....**S-12**

Fig. S8.....**S-13**

Fig. S9.....**S-14**

Fig. S10.....**S-15**

Fig. S11.....**S-16**

Fig. S12.....**S-17**

Fig. S13.....**S-19**

Fig. S14.....**S-21**

Table S1. .....**S-22**

Table S2. .....**S-23**

References.....**S-24**

Experimental section

Reagents

Silver nitrate ($AgNO_3$), nitric acid (HNO_3), bismuth nitrate pentahydrate ($Bi(NO_3)_3·5H_2O$), dimethylformamide (DMF), sodium hydroxide (NaOH), and ethanol absolute were obtained from Sinopharm Chemical Reagent Co., Ltd. Titanium carbide dispersion was purchased from Foshan Xinxi Technology Co., Ltd. The MC-RR aptamer was purchased from Sangon Biological Engineering (Shanghai) Co., Ltd. with the following sequence: 5′-CAG CTC AGA AGC TTG ATC CTA CTG CCC TTC AAT GTT CAC TCC TGT TTC CTG ATC TTT GTC GAC TCG AAG TCG TGC ATC TG-3′.

Apparatus

Scanning electron microscope (SEM) images were obtained using a JEOL scanning electron microscope (JSM-6360LA, Japan). X-ray diffraction (XRD) data were studied using a Max-2000 (Rigaku Co., Ltd, Japan), and X-ray photoelectron spectroscopy (XPS) was tested using an X-ray photoelectron spectroscopy analyzer (250Xl Thermo Fisher Scientific, USA). The UV-vis diffuse reflectance spectrum (DRS) were performed using a Shimadzu UV-3600 spectrometer (Japan). All the electrochemical tests were conducted on a CHI660E electrochemical workstation (Chenhua Instruments Co., Shanghai, China). The PEC performance was tested using a 500 W xenon lamp (CEL-S500, Au Light, Beijing, China).

Preparation of Ag_3BiO_3 nanoparticles

Firstly, 3 mmol of $AgNO_3$ was dissolved in 30 mL of deionized water to obtain

the colorless solution. Next, 2 mL of concentrated nitric acid and 1 mmol of $Bi(NO_3)_3 \bullet 5H_2O$ were added into 10 mL of pure water under stirring conditions. The two solutions were then mixed, and 10 mL of 5 M NaOH solution was then added to the solutions drop by drop. Afterwards, the suspension was put into the stainless steel autoclave and heated at 180 °C for 12 h. After it naturally cooled to room temperature, all deposits were collected and then washed with distilled water and ethanol with several times. Ag_3BiO_3 powder was finally obtained by drying at 60 °C for 12 h.

Fabrication of the photoanode and cathode

The ITO electrodes underwent a 30-minute cleaning process in a 1 M NaOH solution, followed by subsequent rinsing with ultrapure water and ethanol. Then 20 μL of Ag_3BiO_3 dispersion (2 mg/mL) and different amounts of Ti_3C_2 dispersion (0.5 mg/mL) were coated on the ITO surface (1 cm^2), and then the electrode was dried at 60 °C, denoted as Ag_3BiO_3/Ti_3C_2/ITO photoanode.

The porous gas diffusion electrode treated with polytetrafluoroethylene hydrophobicity was used as an air self-breathing cathode. The preparation method was as follows: firstly, 0.1 g platinum black, 0.5 g Nafion perfluororesin solution (5 wt%), 5 mL ethanol and 5 mL pure water were mixed under ultrasonic vibration for 30 min. After that, the prepared catalyst solution was sprayed with the pneumatic spray gun on the carbon paper loaded with carbon nanoparticles and treated with PTFE hydrophobicity, and then the sample was heated at 80 °C for 30 min. The amount of the prepared cathode platinum black was about 1.0 mg/ cm^2.

Fabrication of self-powered aptasensor

20 μL MC-RR aptamer solution (2 μM) was dropped on the resultant Ag_3BiO_3/Ti_3C_2/ITO photoanode, and the aptamers were incubated overnight at room temperature. Subsequently, the aforementioned electrode was cleansed with a 0.1 M buffer solution to eliminate any excess non-adsorbed aptamer. The air self-breathing cathode and the photoanode apta/Ag_3BiO_3/Ti_3C_2/ITO were put into a quartz cell to construct a self-powered sensing device. To achieve the detection of MC-RR, the photoanode apta/Ag_3BiO_3/Ti_3C_2/ITO was subjected to incubation with MC-RR solutions at ambient temperature for 20 minutes. The constructed photoelectrodes were then cleaned with ultrapure water before being used to detect MC-RR.

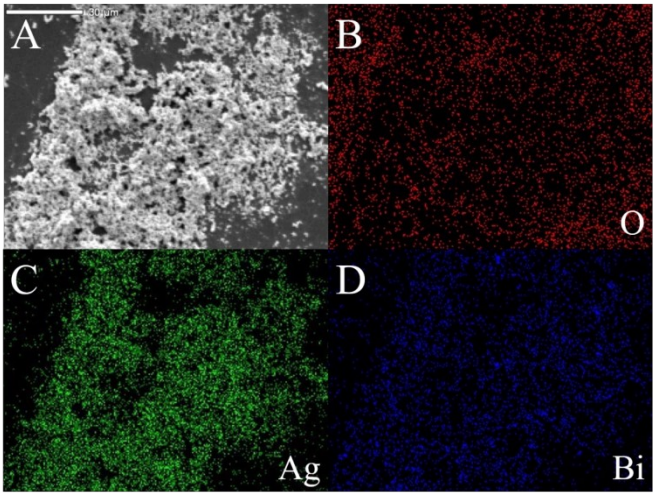

Fig. S1 Elemental mapping analysis of the Ag_3BiO_3.

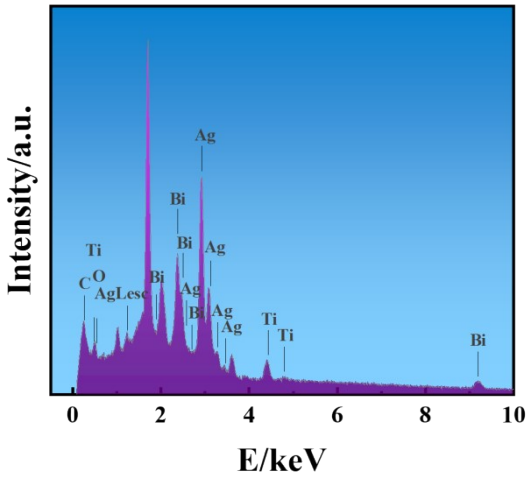

Fig. S2 EDS of Ag_3BiO_3/Ti_3C_2 nanocomposites.

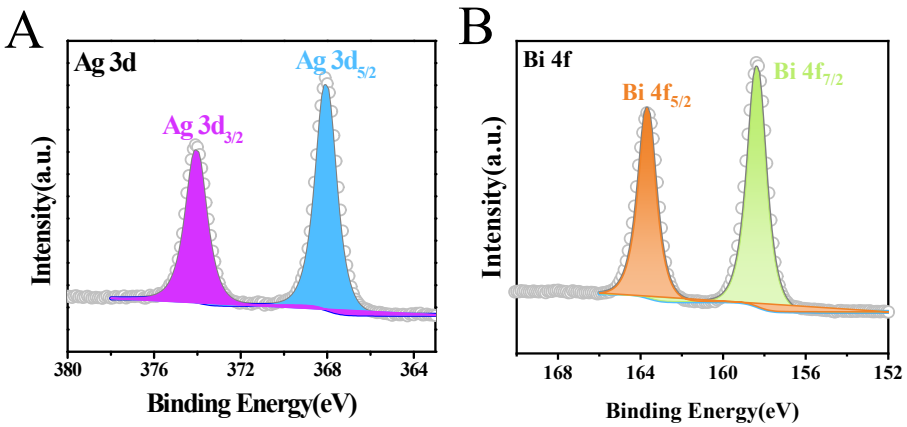

Fig. S3 High-resolution XPS spectra of (A) Ag 3d, and (B) Bi 4f of Ag_3BiO_3/Ti_3C_2 nanocomposites.

The high-resolution XPS spectrum of Ag 3d (Fig. S3A) displayed the peaks centered at 374.0 and 368.0 eV, which were consistent with Ag $3d_{3/2}$ and $3d_{5/2}$, respectively.[1] Fig. S3B presented the high-resolution XPS spectrum of Bi 4f. As can be seen, the binding energies of Bi $4f_{5/2}$ and $4f_{7/2}$ were clearly observed at 163.6 and 158.4 eV, ascribing to Bi^{3+} in Ag_3BiO_3.[2]

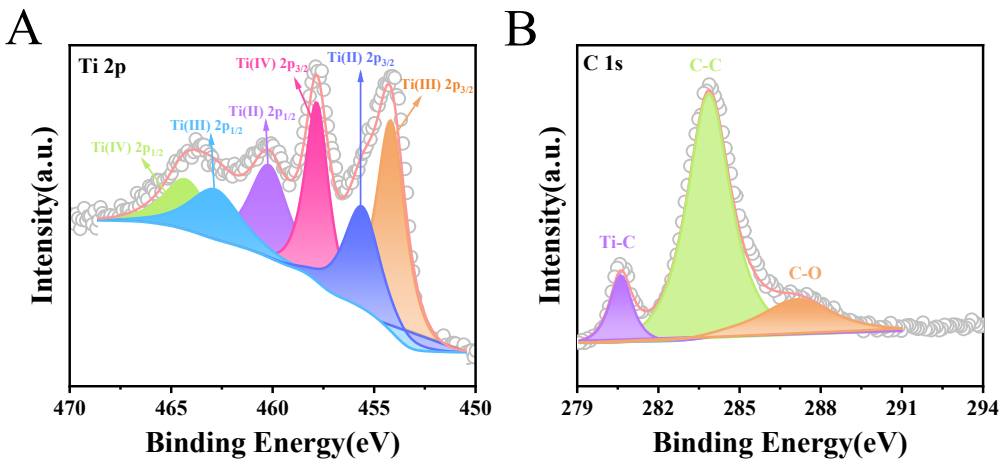

Fig. S4 High-resolution XPS spectra of (A) Ti 2p, and (B) C 1s of Ag_3BiO_3/Ti_3C_2 nanocomposites.

The deconvoluted Ti 2p XPS spectrum (Fig. S4A) could be divided into six peaks at 464.9, 462.7, 460.8, 458.9, 456.2, and 454.6 eV, which were attributed to Ti (IV), Ti (III) $2p_{1/2}$, Ti (II) $2p_{1/2}$, Ti (IV) $2p_{3/2}$, Ti (II) $2p_{3/2}$, and $2p_{1/2}$Ti (III) $2p_{3/2}$, respectively.[3,4] Specifically, the C 1s (Fig. S4B) located at 281.5, 284.8 and 286.4 eV were the characteristic peaks of Ti-C, C-C and C-O, which were the typical bonding of pure Ti_3C_2 MXene.[2] All these results further demonstrated the successful fabrication of Ag_3BiO_3/Ti_3C_2 nanocomposites.

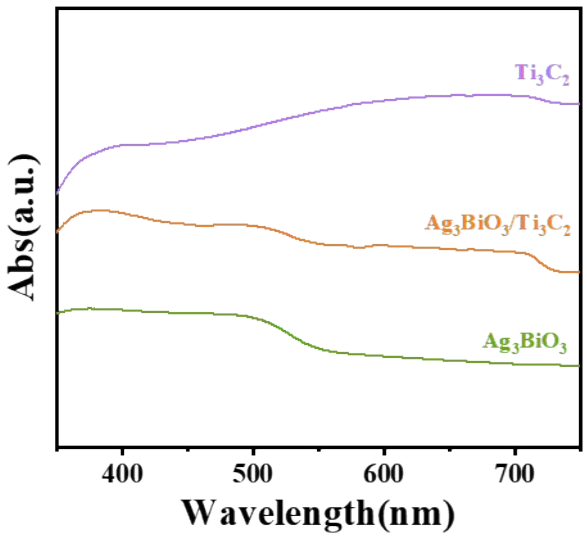

Fig. S5 UV-Vis diffuse reflectance spectra of Ag_3BiO_3, Ti_3C_2 and Ag_3BiO_3/Ti_3C_2 nanocomposites.

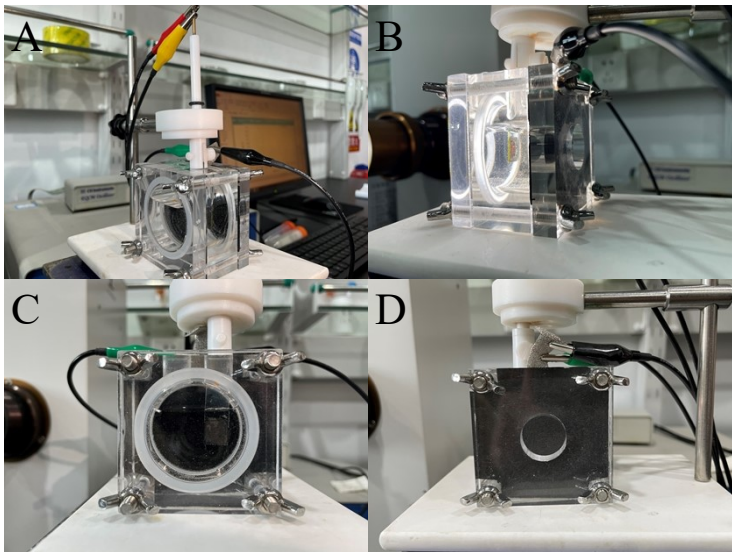

Fig. S6 Digital photos of the entire device based on self-breathing light response self-powered sensor.

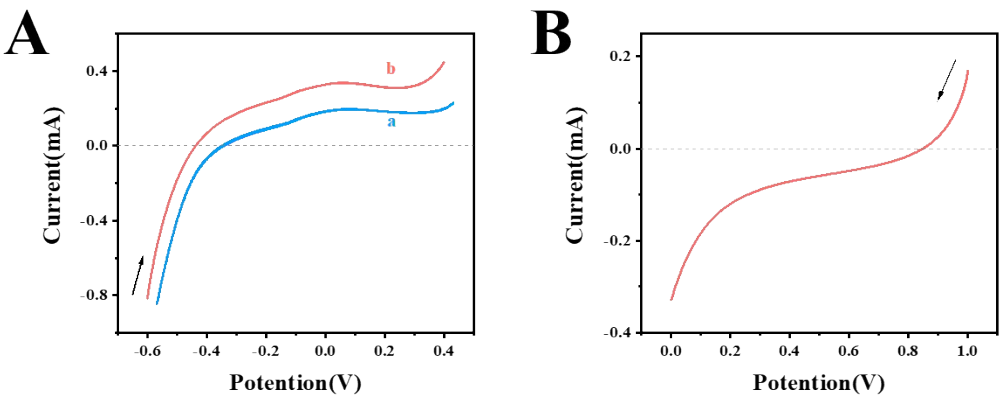

Fig. S7 (A) The photoanodic polarization curves of Ag_3BiO_3/Ti_3C_2/ITO under dark (a) and illuminated (b) conditions; (B) the polarization curves of cathode Pt/C.

In Fig. S7A, the initial oxidation potential (-0.42 V) of Ag_3BiO_3/Ti_3C_2/ITO under light conditions was lower than that of Ag_3BiO_3/Ti_3C_2/ITO under dark conditions (-0.34 V). Whereas, the reduction potential of the Pt/C breathing layer appeared at 0.21 V (Fig. S7B, ESI†). Obviously, the Ag_3BiO_3/Ti_3C_2/ITO and Pt/C breathing layers displayed a large potential difference, and the thermodynamic practicability of the self-powered PEC system was confirmed.[5]

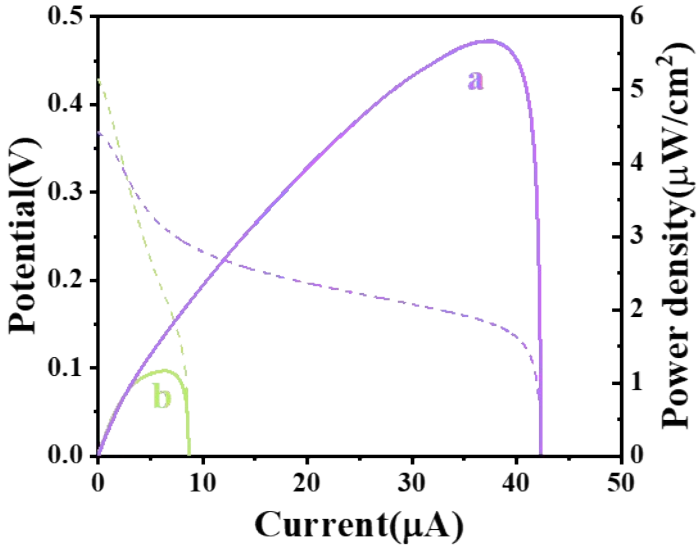

Fig. S8 V-I and P-I curves of the self-powered system by using Ag_3BiO_3/Ti_3C_2 as photoanode, Pt/C self-breathing configuration as cathode (a) and Pt/C/ITO as cathode (b).

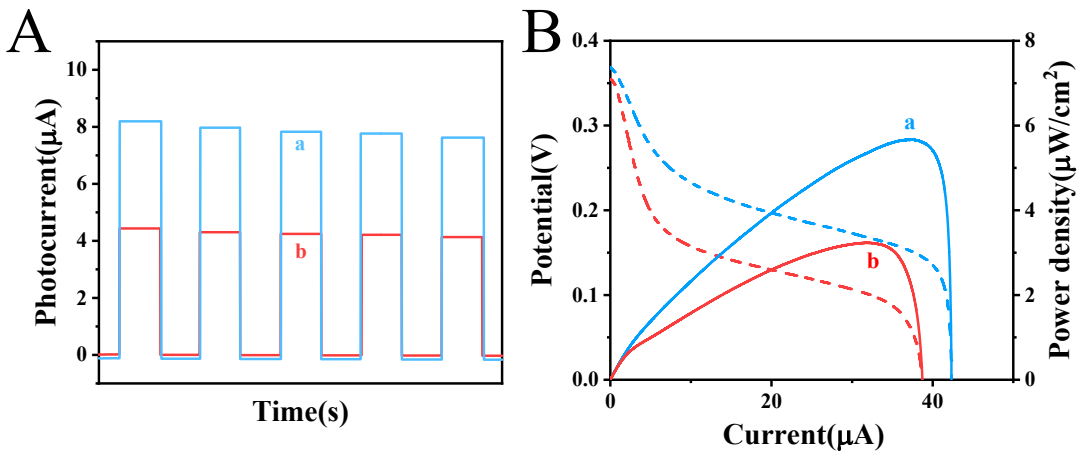

Fig. S9 (A) Photocurrent responses and (B) V-I and P-I curves of the self-powered system prepared with Ag_3BiO_3/Ti_3C_2 as photoanode and Pt/C self-breathing cathode in the air (a) and nitrogen atmosphere (b).

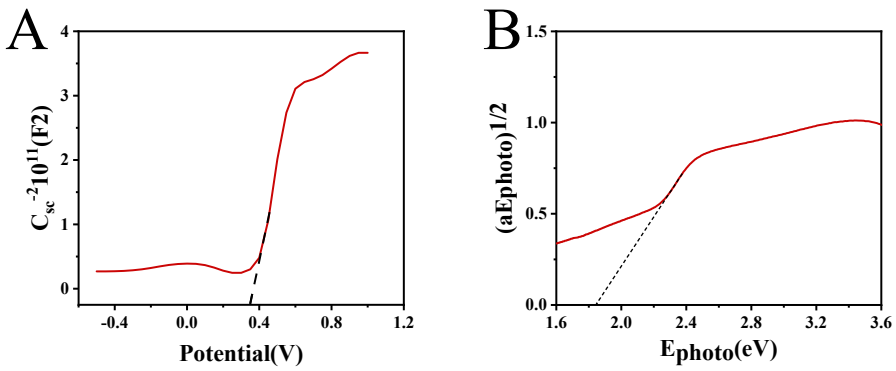

Fig. S10 (A) Mott-Schottky plot of Ag_3BiO_3; (B) Tauc-Plot plot of Ag_3BiO_3.

The following formula can be used to compute the valence band (VB) and conduction band (CB) of Ag_3BiO_3: $E_{VB} = E_{CB} + E_g$.[6] The E_{CB} of Ag_3BiO_3 could be determined by the electrochemical Mott-schottky experiments, and the value could be observed as 0.34 eV (Fig. S10A). By drawing the Tauc diagram of Ag_3BiO_3 based on the curve of hν between $(\alpha h\nu)^{1/2}$, the band gap E_g of Ag_3BiO_3 was determined as 1.84 eV (Fig. S10B). Thus, the E_{VB} of Ag_3BiO_3 could be calculated as 2.18 eV.

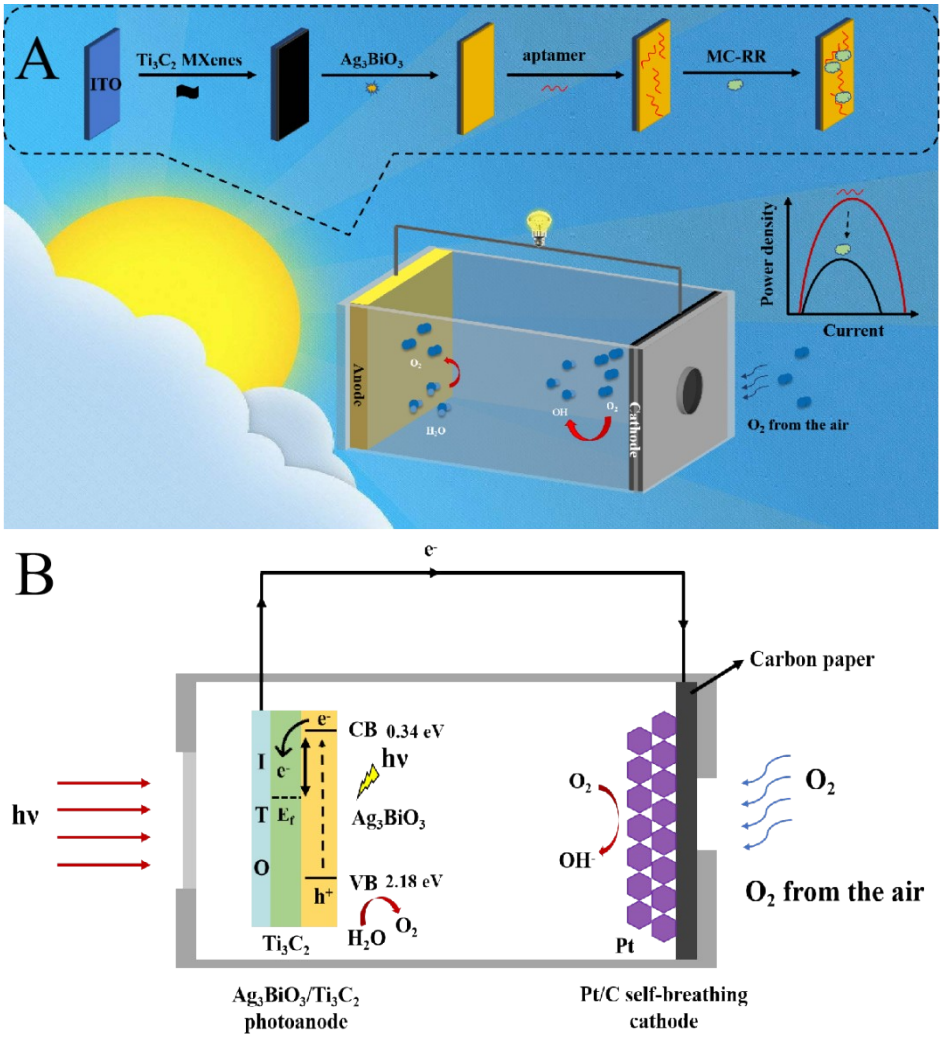

Fig. S11 Schematic diagram of the preparation of self-powered aptasensor based on Ag_3BiO_3/Ti_3C_2/ITO.

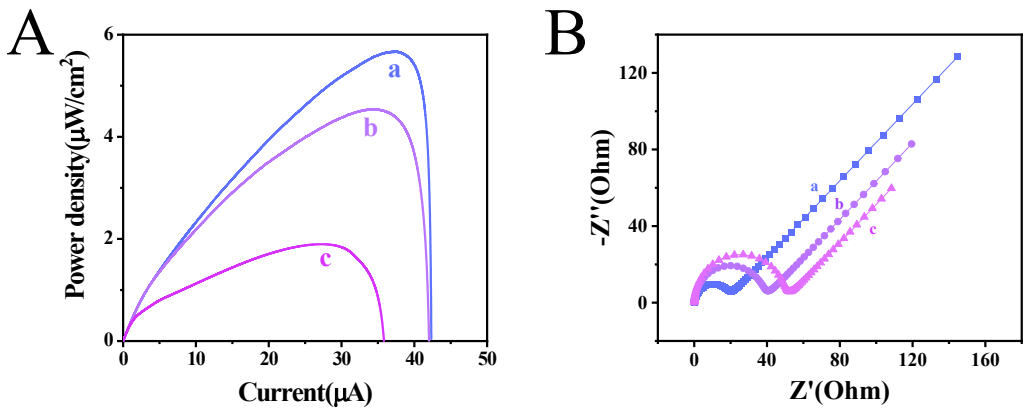

Fig. S12 (C) P-I curves of the PFC system and (D) EIS spectra of aptamer sensors using different photoanodes: Ag_3BiO_3/Ti_3C_2/ITO (a), aptamer/Ag_3BiO_3/Ti_3C_2/ITO (b) and MC-RR/aptamer/ Ag_3BiO_3/Ti_3C_2/ITO (c).

The P-I curves during the construction process were depicted in Fig. S12A. The Ag_3BiO_3/Ti_3C_2/ITO photoanode and Pt/C self-breathing layer cathode PFC system (curve a) demonstrated impressive power output performances. After the introduction of aptamer, the power of the PEC sensor (curve b) reduced dramatically. This could stem from the limited conductivity of the aptamer, which hindered efficient charge transfer across the interface.[7] The appearance of the target triggered the formation of the MC-RR aptamer complex (curve c), significantly impeding electron transfer due to steric hindrance on the electrode surface, thereby leading to a decrease in power output performance.[8] EIS tests were conducted to gain a deeper insight into the interfacial charge transfer dynamics during the fabrication process. As shown in Fig. S12B, the Ag_3BiO_3/Ti_3C_2/ITO photoanode exhibited a small resistance (curve a). Owing to the electrostatic repulsion between the aptamer and $[Fe(CN)_6]^{3-/4-}$, there was a notable increase in the R_{et} value following the addition of the aptamer (as seen in curve b), demonstrating the successful assembly of the aptamer onto the

Ag_3BiO_3/Ti_3C_2/ITO photoanode. Upon introducing MC-RR into the system, the R_{et} of MC-RR/aptamer/Ag_3BiO_3/Ti_3C_2/ITO (curve c) further increased, confirming the assembly of the MC-RR-aptamer complex.[8] The aforementioned analysis aligns with the PEC performance observed during the sensor's construction process, demonstrating the successful construction of the self-powered PEC sensor.

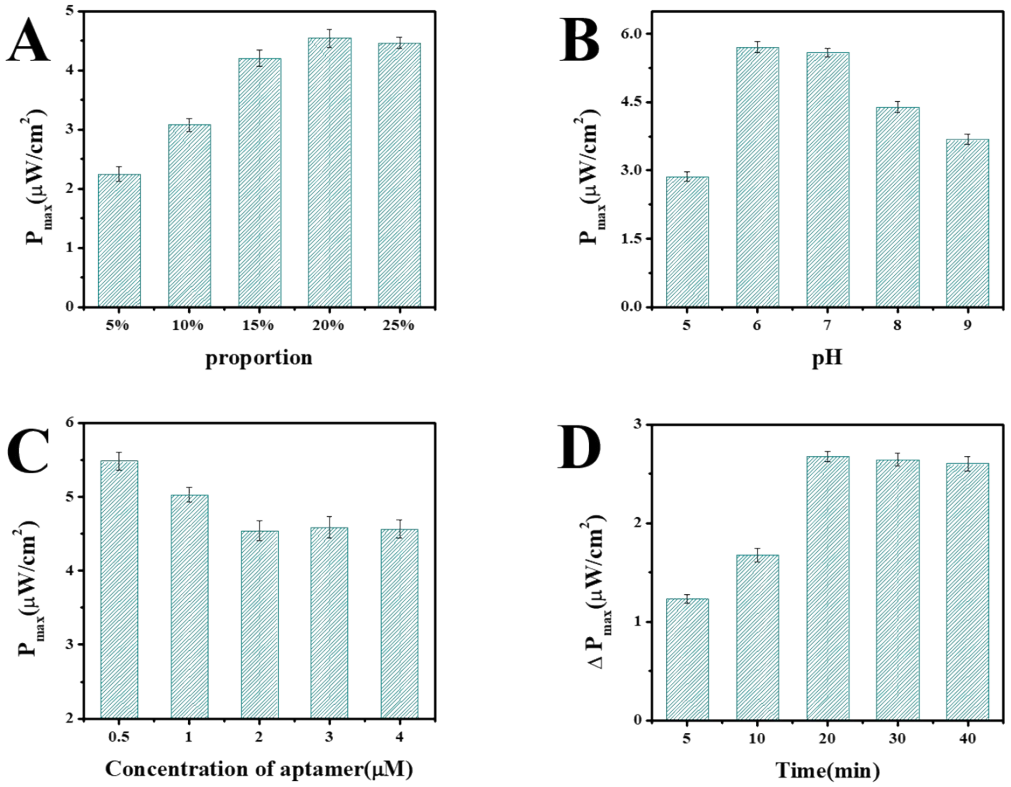

Fig. S13 (A) P_{max} of Ag_3BiO_3/Ti_3C_2/ITO Photoanodes with Different Ratios of Ti_3C_2; (B) Effect of different pH on the P_{max} of the sensor; (C) Effect of aptamer concentration on the ΔP_{max} of the sensor; (D) ΔP_{max} of anode electrode in different incubation time with 10^{-12} M MC-RR.

In order to achieve the high-performance of the self-powered sensor, several experimental conditions have been optimized, including the ratio of Ti_3C_2, pH, aptamer concentration, and incubation time. Firstly, the effect of different ratios of Ti_3C_2 on the performance of the sensor was investigated. As shown in Fig. S13A, the P_{max} of the power density increased continuously as the proportion of Ti_3C_2 increased from 5% to 20%. When the proportion of Ti_3C_2 further increased, the P_{max} no longer changed significantly. Therefore, the optimum ratio of Ti_3C_2 for the photoanode was 20%. Secondly, the effect of different pH values on the power density P_{max} of the self-

powered sensor was also investigated. Fig. S13B showed that P_{max} increased with pH increased from 5 to 6, and then P_{max} gradually decreased with the pH further increased to 9. Therefore, pH = 6 was chosen as the optimal condition. The effect of different aptamer concentrations on the power density of the self-powered sensor was also investigated in Fig. S13C. As can be seen, the P_{max} value gradually decreased when the aptamer concentration was increased from 0.1 μmol/L to 2.0 μmol/L. Then the P_{max} values tended to remain unchanged with aptamer concentration further increase. Therefore, the optimal aptamer concentration was 2.0 μmol/L. Fig. S13D presented the effect of incubation time on system power density. It is obvious that the ΔP_{max} value increased significantly with the incubation time increasing in the range of 5 to 20 min, and then reached a maximum value. When the incubation time exceeded 20 min, the power density remained unchanged. Therefore, 20 min was the suitable time for this experiment.

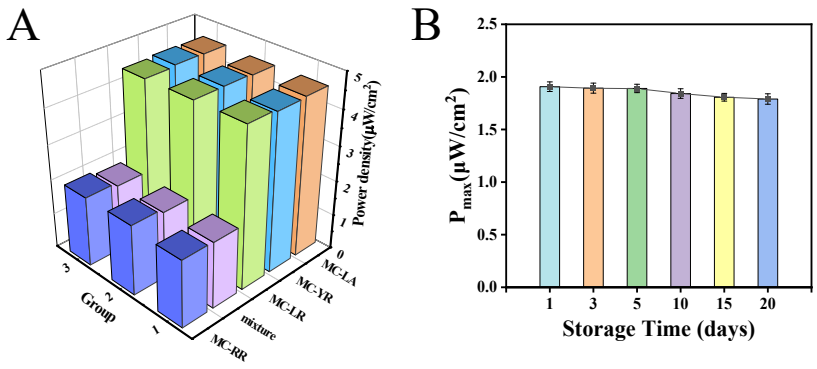

Fig. S14 (A) Selectivity and (B) Stability of the developed sensor.

Table S1 Comparison of different methods for the determination of MC-RR.

Method	Linear range (M)	Detection limit(M)	Ref.
SERS Detection	1.0×10^{-12}-5.0×10^{-7}	0.8×10^{-12}	9
biosensor	0.9×10^{-14}-0.3×10^{-8}	2.9×10^{-10}	10
chemiluminescence aptasensor	1.0×10^{-10}-7.0×10^{-7}	3.3×10^{-11}	11
UHPLC-MS/MS	4.8×10^{-11}-9.6×10^{-10}	2.1×10^{-9}-4.0×10^{-13}	12
Self-powered PEC aptasensor	1.0×10^{-15}-1.0×10^{-10}	1.05×10^{-16}	This work

Table S2 Analytical results of MC-RR based on the developed sensor.

Sample	Added (fM)	Detected (fM)	Recovery (%)	RSD (%) (n=3)
Tap water	0	—	—	—
	0.5	0.48	96.0	3.1
	1.0	0.98	98.0	3.9
Pond water	0	—	—	—
	0.5	0.52	104.0	4.9
	1.0	1.01	101.0	4.4

References

1. D. Jiang, M. Wei, X. J. Du, M. Qin, X. L. Shan, Z. D. Chen, Chem. Eng. J., 2022, **430**, 132771.
2. H. X. Liao, C. H. Jin, Y. Zhou, Y. Q. Chai, R. Yuan, Anal. Chem., 2019, **91**, 11447-11454.
3. S. Feizpoor, A. Habibi-Yangjeh, R. Luque, Environ. Res., 2022, **215**, 114315.
4. T. Cai, L. L. Wang, Y. T. Liu, S. Q. Zhang, W. Y. Dong, H. Chen, X. Y. Yi, J. L. Yuan, X. N. Xia, C. B. Liu, S. L. Luo, Appl. Catal., B, 2018, **239**, 545-554.
5. J. B. Li, D. Yan, S. J. Hou, Y. Q. Li, T. Lu, Y. F. Yao, L. K. Pan, J Mater Chem A, 2018, **6**, 1234-1243.
6. X. L. Yao, J. Gao, K. Yan, Y. X. Chen, J. D. Zhang, Anal. Chem., 2020, **92**, 8026-8030.
7. J. Wei, Q. Q. Hu, Y. Gao, N. Hao, J. Qian, K. Wang, Anal. Chem., 2021, **93**, 12690-12697.
8. H. L. Ding, D. Jiang, X. J. Du, Z. L. Zhang, J. H. Jiang, X. L. Shan, W. C. Wang, H. Shiigi, Z. D. Chen, Anal. Chem., 2023, **95**, 12595–12599.
9. X. J. Luo, X. J. Zhao, G. Q. Wallace, M. H. Brunet, K. J. Wilkinson, P. Wu, ACS Appl. Mater. Interfaces, 2021, **13**, 6545-56.
10. Y. Shi, J. Z. Wu, Y. J. Sun, Y. Zhang, Z. W. Wen, H. C. Dai, *Biosens. Bioelectron.*, 2012, **38**, 31-6.
11. B. R. Liu, X. H. Li, S. M. Liu, X. Hun, *Microchem. J.*, 2019, **145**, 648-54.
12. X. Y. Liu, S. Q. Gao, X. Y. Li, H. Wang, X. W. Ji, Z. E. Zhang, *Ecotoxicol. Environ. Saf.*, 2019, **176**, 20-6.